Talanta 158 (2016) 142–151

Contents lists available at ScienceDirect

Talanta

journal homepage: www.elsevier.com/locate/talanta

Electrochemiluminescence biosensor for determination of organophosphorous pesticides based on bimetallic Pt-Au/multi-walled carbon nanotubes modified electrode

Shan Shan Miao [a,b,1], Mei Sheng Wu [a,1], Li Ya Ma [a], Xiao Jing He [a], Hong Yang [a,b,*]

[a] Jiangsu Key Laboratory of Pesticide Science, College of Sciences, Nanjing Agricultural University, Nanjing 210095, China
[b] State & Local Joint Engineering Research Center of Green Pesticide Invention and Application, Nanjing Agricultural University, Nanjing 210095, China

ARTICLE INFO

Article history:
Received 19 February 2016
Received in revised form
10 May 2016
Accepted 11 May 2016
Available online 13 May 2016

Keywords:
Organophosphorous pesticides
Acetylcholineesterase
Choline oxidase
Electrochemiluminescence
Luminol
Pt-Au NPs
MWCNTs

ABSTRACT

A novel and highly sensitive electrochemiluminescence (ECL) biosensing system was designed and developed for individual detection of different organophosphorous pesticides (OPs) in food samples. Bimetallic Pt-Au nanoparticles were electrodeposited on multi-walled carbon nanotubes (MWNTs)-modified glass carbon electrode (GCE) to increase the surface area of electrode and ECL signals of luminol. Biocomposites of enzymes from acetylcholinesterase and choline oxidase (AChE and ChOx) were immobilized onto the electrode surface to produce massive hydrogen peroxides (H_2O_2), thus amplifying ECL signals. Based on the dual-amplification effects of nanoparticles and H_2O_2 produced by enzymatic reactions, the proposed biosensor exhibits highly sensitivity. The proposed biosensing approach was then used for detecting OPs by inhibition of OPs on AChE. Under optimized experimental conditions, the ECL intensity decreased accordingly with the increase in concentration of OPs, and the inhibition rates of OPs were proportional to their concentrations in the range of 0.1–50 nmol L^{-1} for malathion, methyl parathion and chlorpyrifos, with detection limit of 0.16 nmol L^{-1}, 0.09 nmol L^{-1} and 0.08 nmol L^{-1}, respectively. The linearity range of the biosensor for pesticide dufulin varied from 50 to 500 nmol L^{-1}, with the detection limit of 29.7 nmol L^{-1}. The resulting biosensor was further validated by assessment of OPs residues in cabbage, which showed a fine applicability for the detection of OPs in the realistic sample.

1. Introduction

Organophosphorus pesticides (OPs) are a large group of pesticides and widely used in agronomic practice for killing insects and protecting crop production [1,2]. As toxic chemicals once OPs contaminate humans and animals, the visual and nervous system, and sensory or cognitive function can be seriously impaired [3]. It was reported that OPs or their active metabolites can exert their detrimental effects by blocking the enzyme activity of acetylcholinesterase (AChE), which in turn leads to accumulation of the neurotransmitter acetylcholine (Ach) in synapses as well as over-stimulation of the post-synaptic cholinergic receptors with a consequence of neurotoxicity [4,5]. Considering the environmental security and risk of OPs, it is of great importance and urgency to develop an accurate, sensitive, and rapid method to monitor the realistic environmental and food contamination. Up to now, various methodologies have been developed for assessment of OPs, such as high performance liquid chromatography (HPLC) [6], gas chromatography (GC) [7], chemiluminescence [8], and thin-layer chromatography (TLC) [9]. However, most of the methods require expensive equipments and complicated sample pretreatment. Besides, vast organic solvents used for OPs extraction from samples may not be cost-effective. Therefore, establishing a low-cost, high efficient and easy-to-use method for OPs detection is essentially important.

Recently, electrochemiluminescence (ECL) has been emerging as an alternative to the conventional methods and is able to meet demands of high sensitivity, low background signal and simple instrumentation [10]. It takes an advantage of technically merged chemiluminescence and electrochemistry [11,12] with generation of species at electrode surfaces where electron-transfer reactions occur to form excited states of light emitting [13,14]. A variety of ECL reagents such as luminol [15,16], semiconductor nanocrystals (NCs)-based ECL system [17] and tris (2,2′-bipyridine) ruthenium (II) $\left(Ru(bpy)_3^{2+}\right)$ [18,19] have been used to develop sensitive biosensor. Recently, luminol has become one of the most popular ECL reagents on account of low oxidation potential, high emission yields and inexpensive reagent consumption. The reactive oxygen

* Correspondence to: College of Sciences, Nanjing Agricultural University, Weigang No.1, Chemistry Building, Nanjing 210095, China.
E-mail address: hongyang@njau.edu.cn (H. Yang).
[1] The authors made equal contribution to the study.

http://dx.doi.org/10.1016/j.talanta.2016.05.030
0039-9140/

species (ROSs) have been demonstrated to improve the ECL performance of luminol in neutral medium [20]. As one of the ROSs, hydrogen peroxide (H_2O_2) is a highly reactive species owning to its presence of unpaired valent shell electron. H_2O_2 in the luminol-H_2O_2 system was found to enhance the ECL of luminol efficiently under various experimental conditions [21]. Such intensification could reduce the limitation of ECL of luminol, such as extension of practicable pH window, need for strong alkaline solution and requirements for high exciting potential to avoid possible interference [22]. Recent studies have shown that AChE-based inhibitory biosensors served as an alternative for OPs analysis [23]. The activity of AChE has been generally used as a quantitative indicator of OPs measurement [24]. Choline is the product of the enzymatic reaction. It can be oxidized on the surface of electrode and generate electrochemical signals. Upon addition of OPs, the enzyme activity of AChE would be inhibited, which can induce the decrease of electrochemical signals. However, the product would be different when a two-enzyme approach (AChE and ChOx) was employed in assembling the biosensor. Since the hydrolysis product of AChE, choline was further oxidized by ChOx in the presence of oxygen, H_2O_2 is produced [25,26]. Similarly, addition of OPs would inhibit the AChE activity, which in turn reduces H_2O_2, and as a consequence would weaken the ECL signal of luminol. In this regard, biosensor could be employed based on the ECL of luminol intensified by H_2O_2. To the best of our knowledge, there has been no report on using luminol-H_2O_2 approach for OPs assessment.

In order to achieve sensitive determination, nanometer-scale materials have been used in fabrication of biosensors for their large surface area, high loading capacity and uniform pore structure [3]. A previous report indicated that multi-walled carbon nanotubes (MWCNTs) displayed a fast heterogeneous charge transfer and possessed electrocatalytic properties due to the edge plane sites in MWCNTs occurring at the ends and along the tube axis [27]. Metal nanoparticle (NP) is another kind of popular material owning to its high surface-to-volume ratio and high surface energy. For example, Pt NPs and Au NPs showed unusual physical and chemical properties, depending on their size and shape [28]. Potential application of Pt and Au in electrochemistry, electron-transfer and ECL reactions has been investigated [22,29,30], and the promoted effect on ECL signals of luminol-H_2O_2 system from Au NPs was reported as well [31]. Pt NPs can not only catalyze ECL of luminol molecules in solution but also enrich luminol molecules on the surface of nanoparticles [32]. Electrodes modified with metal NPs such as Au or Pt were showed to enhance the ECL emission of luminol by 2–3 orders as compared to the original bare electrodes [21]. Inspired by the superiorities of above nanomaterials, here we present a novel biosensor modification strategy. We utilized the unique synergy properties of Au-Pt bimetallic NPs and MWCNTs to improve biosensor performance and avoid the deficiency and limitation of single nanomaterial. The novel biosensor had been developed by electrodeposition of the Pt-Au bimetallic NPs on the MWCNTs modified glass carbon electrode (GCE). The biocomposites AChE & ChOx were coimmobilized on the Pt-Au/MWCNT-modified GCE by cross-linking the enzymes and modified GCE through cysteine. Because H_2O_2 was generated in the bioenzyme system, the ECL signal of luminol was significantly amplified on AChE&ChOx/Pt-Au/MWCNT/GCE. Herein, the OPs malathion, methyl parathion, chlorpyrifos and dufulin were chosen as the inhibitors of AChE. On the base of the effects of OPs on the ECL signal of luminol, a new rapid and sensitive luminol-based ECL approach was developed for OPs detection.

2. Experimental

2.1. Materials and chemicals

The organophosphorous pesticide dufulin (99%) was obtained from Center for Research and Development of Fine Chemicals of Guizhou University. Malathion (95%), chlorpyrifos (99%) and methyl parathion (99%) were obtained from Syngenta Nantong Crop Protection Co., Ltd. MWCNTs (10–20 nm diameter, length 10–30 μm, and >95% purity) were obtained from JC NANO, Inc. (China). Chloroauric acid ($HAuCl_4 \cdot 4H_2O$, 47.8%) and chloroplatinic acid ($H_2PtCl_6 \cdot 6H_2O$, 37.5%) were purchased from Aladdin Co., Ltd. L-Cysteine (99%) was purchased from J & K Chemical Co., Ltd. 1-(3-Dimethylaminopropyl)-3-ethylcarbodiimide hydrochloride (EDC), N-Hydroxysuccinimide (NHS), luminol (>97%), AChE (EC 3.1.1.7, type VI-S; from electric eel; activity 149 U/mg solid), ChOx (EC 1.1.3.17, from *Alcaligenes* sp. activity 14 U/mg solid), and acetylcholine chloride (ATCI) were purchased from Sigma-Aldrich Co., Ltd. (USA). The luminol stock solution (20 mmol L^{-1}) was prepared by dissolving the required amounts of luminol in 0.2 mol L^{-1} sodium hydroxide solution and stored in a light-proof environment. All other chemicals from commercial source were of analytical grade. Phosphate buffer solutions (PBS, 0.1 mol L^{-1}) with various pH values were prepared by mixing stock standard solutions of K_2HPO_4 and KH_2PO_4. Double-distilled water was used throughout the experiments.

2.2. Apparatus

The electrochemiluminescence was measured on a model MPI-E ECL working station (Xi'an Remex Analysis Instruments Co., Ltd. China). A conventional three-electrode configuration was employed, consisting of a glassy carbon electrode (GCE, Φ=3 mm) served as the working electrode, a saturated calomel electrode (SCE) as the reference electrode, and a platinum wire as the counter electrode. The voltage of the photomultiplier tube (PMT) was set at 800 V in the process of detection. The electroanalytical measurements such as cyclic voltammetry (CV), amperometric i-t curve and electrochemical impedance spectroscopy (EIS) were performed with a CHI660E electrochemical analyzer. A field emission scanning electron microscope (FESEM, S-4800, Hitachi, Japan) operated at an accelerating voltage of 15.0 kV and an energy dispersive X-ray spectrometer (EDX) attached to the FESEM were used to characterize the surface of electrodes.

2.3. Preparation of Pt-Au/MWCNT modified electrode

The outer surfaces of MWCNTs were grafted with –COOH to enhance the dispersion and stability according to the previous report [33]. Briefly, MWCNTs (400 mg) was refluxed in a H_2SO_4-HNO_3 blend acid (3/1, V/V) at 95 °C for 20 h. The mixture was centrifuged and repeatedly washed with double-distilled water to neutrality and dried under N_2. The black solid obtained was denoted as MWCNTs-COOH.

Prior to modification, the bare GCE was polished to a mirror-like surface with 1, 0.3, and 0.05 μm alumina slurry, rinsed ultrasonically in ethanol and double distilled water for 5 min each time. MWCNTs-COOH (25 mg) and double-distilled water (20 mL) were mixed in a flask with the help of magnetic stirring to form a homogeneous suspension. A certain volume of the resulting suspension was casted onto a GCE and dried at room temperature (denoted as MWCNT/GCE).

After that, Pt-Au was electrodeposited at MWCNT/GCE surface through amperometric i-t curve at −0.2 V for 300 s in deoxygenated solution of 0.5 mol L^{-1} H_2SO_4 solution with 5 mmol L^{-1} H_2PtCl_6. Subsequently, the same procedure was

performed in 0.5 mol L^{-1} H_2SO_4 solution containing 5 mmol L^{-1} $HAuCl_4$ (denoted as Pt-Au/MWCNT/GCE) [26]. For comparison, Pt&Au/MWCNT/GCE, Au/MWCNT/GCE, and Pt/MWCNT/GCE were prepared with the same method in 0.5 mol L^{-1} H_2SO_4 solution containing the mixture of 5 mmol L^{-1} $HAuCl_4$ and 5 mmol L^{-1} H_2PtCl_6, 5 mmol L^{-1} $HAuCl_4$, and 5 mmol L^{-1} H_2PtCl_6, respectively. After electrodeposition, the modified electrodes were gently washed with double distilled water and dried at room temperature.

2.4. Fabrication of the ECL biosensor

For immobilization of the biocomposites AChE-ChOx onto the electrode, the modified electrode was first immersed in 0.02 mol L^{-1} L-cysteine solution at 4 °C for 20 h. The resulting electrode was rinsed thoroughly with double-distilled water. Then, the electrode was immersed in PBS containing 20 mg mL^{-1} EDC and 10 mg mL^{-1} NHS at 37 °C for 1 h to activate the –COOH of L-cysteine. After that, the electrode was rinsed with double-distilled water. Finally, 10 μL of the mixed enzyme solution (0.004 U AChE and 2 U ChOx) was dropped onto the modified GC electrode and allowed to dry overnight at 4 °C. The dried electrode was rinsed with PBS (pH 7.4) to remove loosely bound enzymes and stored at 4 °C (denoted as AChE&ChOx/Pt-Au/MWCNT/GCE).

2.5. ECL measurements

Organophosphorous pesticides malathion, chlorpyrifos, methyl parathion and dufulin were chosen as the representative OPs for AChE inhibition. AChE&ChOx/Pt-Au/MWCNT/GCE was first immersed in PBS (pH 7.4) solution containing different concentrations of standard malathion or other pesticides at 4 °C for 10 min and immersed to the solution of 10 mL pH 8.0 PBS containing 2.0 mmol L^{-1} ATCl and 0.4 mmol L^{-1} luminol to perform cyclic ECL measurement. The potential was ranged within 0.3–0.6 V, with a scan rate 100 mV/s.

2.6. OPs assessment in cabbage

The analytical performance of the proposed biosensor was used to determine the OPs residues in cabbage. The vegetable was chopped and ground. Samples were extracted with 20 mL chloroform and repeated in triplicate. The extracts were pooled and evaporated to dryness under vacuum with a rotary evaporator. The residue was resolved in suitable volumes of PBS (0.1 mol L^{-1}, pH 7.4). The solution was filtered by 0.22 μm nylon membrane and detected for the proposed ECL biosensor. Meanwhile, the spiked recovery test was also carried out to verify the feasibility of the method. Ground cabbage sample was spiked with an appropriate volume of standard malathion (or chlorpyrifos, methyl parathion and dufulin) to obtain the final concentrations of 1, 40 and 100 nmol kg^{-1}, respectively. The final concentrations of dufulin were 100, 250 and 500 nmol kg^{-1}. The spiked samples were incubated and stood for about an hour before extraction. The extraction and analysis were the same as indicated above.

3. Results and discussion

3.1. Principle of the ECL biosensor

Fig. 1 depicts the principle of dual-amplification strategy for OPs detection. Briefly, carboxyl-modified MWCNT was modified on the GCE surface. The bimetallic Pt-Au NPs were deposited, followed by conjugating with AChE&ChOx. In this case, ATCI in ECL detection solution was hydrolyzed into choline and acetate by AChE (Eq. (1)). Choline was further oxidized into betaine and H_2O_2 (Eq. (2)). As a result, the ECL signal of luminal was stimulated by bimetallic NPs and enzyme. When OPs were added, the enzyme activity of AChE was inhibited, and consequently, the ECL signal intensity was declined.

$$\text{Acetylcholine} + H_2O \xrightarrow{\text{AChE}} \text{Choline} + \text{Acetate} \quad (1)$$

$$\text{Choline} + 2O_2 + H_2O \xrightarrow{\text{ChOx}} \text{Betaine} + 2H_2O_2 \quad (2)$$

3.2. Surface characterization of the prepared electrode

The morphology of the MWCNT/GCE and Pt-Au/MWCNT/GCE was characterized by SEM studies (Fig. 2). The SEM image indicated that the average diameter of MWCNTs was at around 30 nm (Fig. 2A). MWCNTs were well distributed homogeneously on the electrode surface. Most of them were in the form of single tubes or small bundles. After deposition of Pt and Au NPs, a large amount of particles were found to attach on the MWCNTs surface. The sizes of the particles were in the range of 20–50 nm (Fig. 2B).

The EDX analysis was performed to investigate elemental compositions of the modified electrode. The results were illustrated in Fig. 2C. The image pointed to the dominant peaks of Au and Pt, suggesting the successful electrodeposition of Au and Pt on the MWCNT/GCE.

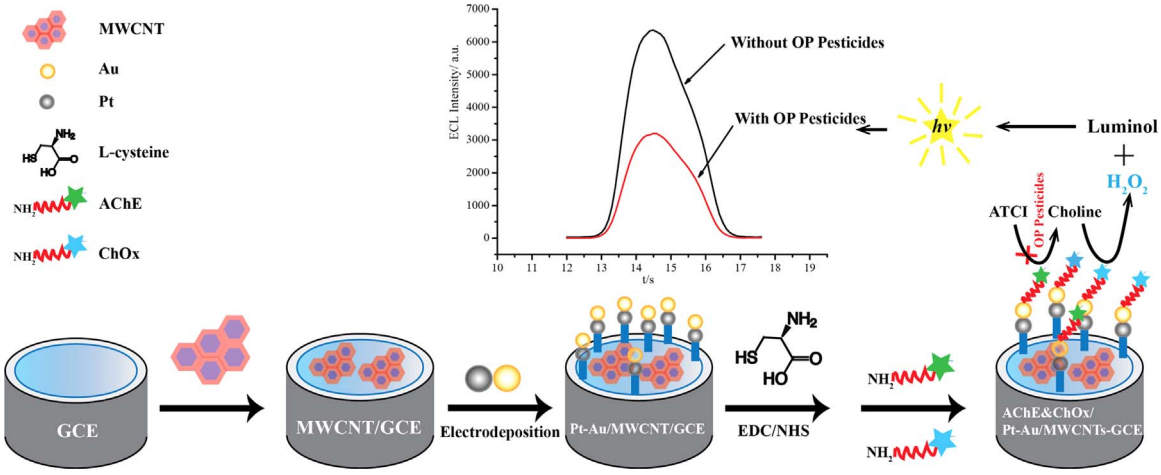

Fig. 1. Schematic illustration of the fabrication of the biosensor and the principle of dual-amplification strategy for OPs detection.

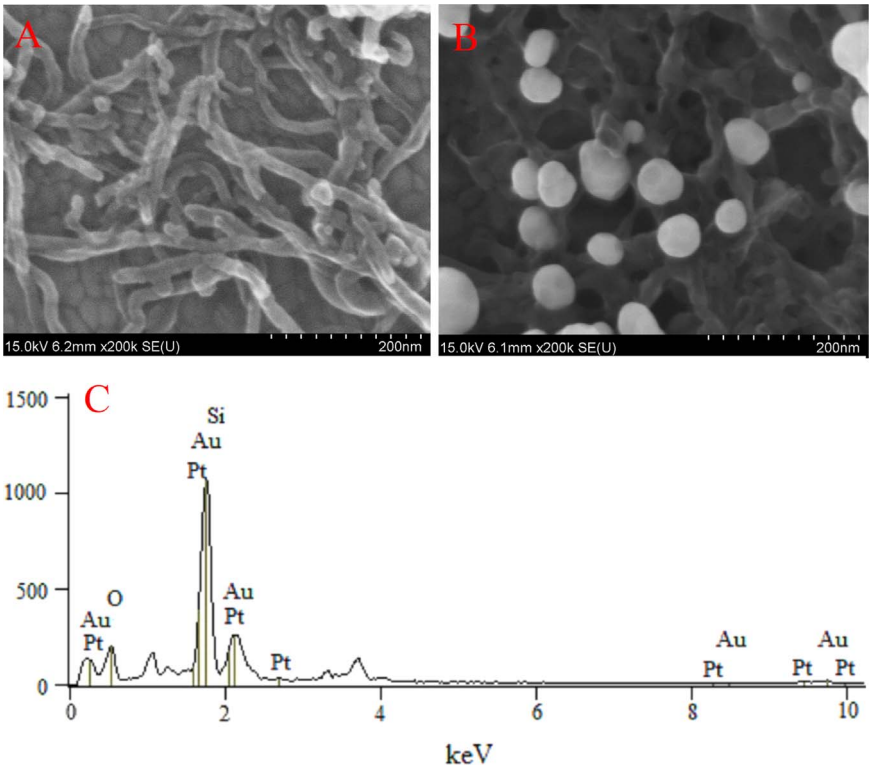

Fig. 2. SEM images of MWCNT (A) and Pt-Au/MWCNT (B). EDX image of Pt-Au/MWCNT (C).

3.3. Electrochemical and ECL behavior of modified electrodes

3.3.1. Electrochemical characterization of modified electrodes

Cyclic voltammetry (CV) and electrochemical impedance spectroscopy (EIS) were used to investigate the electrochemical characteristics of the modified electrodes. The CVs of stepwise modified electrodes in 2 mmol L^{-1} $Fe(CN)_6^{3-/4-}$ containing 0.2 mol L^{-1} KCl solution were showed in Fig. 3A. In case of bare GCE, a well-defined redox peak (current ~51 μA and potential ~0.18 V) with peak-to-peak separation (ΔE_p) of ~69 mV was observed. After deposition of MWCNTs, the redox peak current increased. This could result from the excellent electrochemical conductivity and small dimensional size of MWCNTs [34]. Following the modification of bimetallic Pt-Au NPs, the CV redox peak current (261 μA) was further enhanced. This was due to the high conducting Au and Pt NPs, which behaved as an electron-transfer channel and further improved the conductivity of GCE [35,36]. With the combination of AChE&ChOx onto Pt-Au/MWCNT/GCE surface, an obvious decrease of the redox current was observed, owing to the hindrance of nonconductive multiple enzymes.

EIS was also employed to characterize interface properties of the stepwise assembly of biosensor. The typical impedance spectrum includes a semicircle portion and a linear portion. The semicircle diameter at higher frequencies corresponds to the electron-transfer process, and the linear part at lower frequencies represents the diffusion-limited process [22]. The diameter of semicircle was equivalent to the electron-transfer resistance (R_{et}) [37]. The results of EIS on different electrodes in the presence of 5 mmol L^{-1} $Fe(CN)_6^{3-/4-}$ containing 0.2 mol L^{-1} KCl solution with a frequency range of 1 Hz–100 kHz were illustrated in Fig. 3B. Bare GCE had an obvious semicircle. The R_{et} value was 267 Ω. At MWCNT/GCE, a dramatically decreased semicircle diameter was found. This could be explained by the fact that MWCNTs were immobilized on GCE and the excellent conductivity of MWCNTs could promote electron transfer. After modification with nanoparticles Pt and Au, the Pt-Au/MWCNT/GCE displayed a nearly straight line with very low R_{et}. These results imply that MWCNTs-coated bimetallic Pt-Au NPs acted as good electron conducting materials. That made high electron conduction pathways between anionic $Fe(CN)_6^{3-/4-}$ and the electrode. When compared to the nanocomposites-modified electrode, the semicircle diameter increased with the immobilization of AChE&ChOx biocomposite on the Pt-Au/MWCNT/GCE, with a R_{et} value of 91 Ω.

3.3.2. Electrochemiluminescence characterization of the modified electrodes

To illustrate the dual-amplification effect of the proposed biosensor, we measured ECL behaviors of the modified electrode step by step. No ECL signal was observed on bare GCE (curve a), while both MWCNT/GCE and Pt-Au/MWCNT/GCE showed slight ECL signals (curve b and c) (Fig. 3C). With AChE&ChOx immobilization onto the Pt-Au/MWCNT/GCE, the intensity of ECL peak was considerably increased up to 6179 (curve d). Besides, the electrode showed an excellent stability after 10 cycles with RSD of 2.13% (inset Fig. 3C). To make a comparison, we modified AChE&ChOx on MWCNT/GCE (curve e). It was shown that the ECL signal was only 23.46% that of AChE&ChOx /Pt-Au/MWCNT/GCE (curve d), confirming that the significant enhancement of the ECL signal was not only caused by MWCNTs and bimetal Pt and Au, but also induced by massive anchoring sites provided by bimetallic Pt-Au NPs for immobilization of AChE&ChOx.

We presented the ECL signals of luminol at AChE&ChOx/MWCNT/GCE (a), AChE&ChOx/Pt/MWCNT/GCE (b), AChE&ChOx/Au/MWCNT/GCE (c), AChE&ChOx/Pt&Au/MWCNT/GCE (d), and AChE&ChOx/Pt-Au/MWCNT/GCE (e), respectively (Fig. 3D). The ECL intensity of the modified GCE without electrodeposition was very low (a). After deposition of Pt (b) or Au (c), both ECL responses were enhanced, with the intensity values being 2259 and 3955, respectively. Given that Pt and Au were deposited at the same time (d), the increased ECL signal might be observed, but it was still lower than that at AChE&ChOx/Pt-Au/MWCNT/GCE (e). Therefore, the way of electroplating first in 5 mmol L^{-1} H_2PtCl_6,

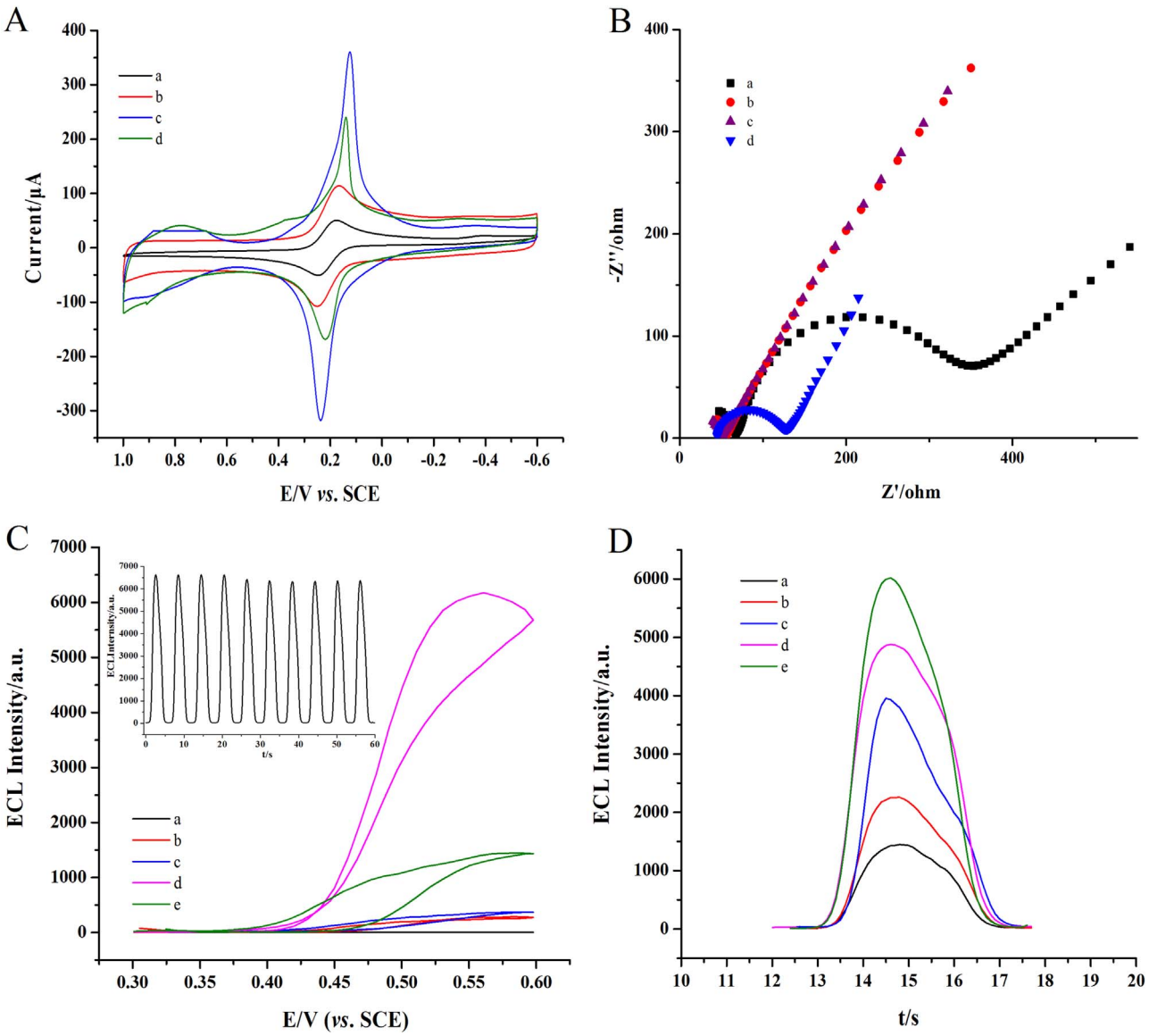

Fig. 3. (A) CVs and (B) EIS for (a) bare GCE, (b) MWCNT/GCE, (c) Pt-Au/MWCNT/GCE, and (d) AChE&ChOx/Pt-Au/MWCNT/GCE in $Fe(CN)_6^{3-/4-}$ solution. (C) ECL response of (a) bare GCE, (b) MWCNT/GCE, (c) Pt-Au/MWCNT/GCE, (d) AChE&ChOx/Pt-Au/MWCNT/GCE and (e) AChE&ChOx/MWCNT/GCE in 10 mL 0.1 M PBS (pH 8.0) with 0.4 mM luminol and 2 mM ATCI. Scan rate: 100 mV/s. The inset shows the stability of the proposed biosensor. (D) Effect of electroplating ways on the ECL intensity with 2 mM ATCI and 0.4 mM luminol in 0.1 M PBS (pH 8), (a) AChE&ChOx/MWCNT/GCE, (b) AChE&ChOx/Pt/MWCNT/GCE, (c) AChE&ChOx/Au/MWCNT/GCE, (d) AChE&ChOx/ Pt&Au/MWCNT/GCE and (e) AChE&ChOx/Pt-Au/MWCNT/GCE.

and the same procedure in 5 mmol L^{-1} $HAuCl_4$ was selected for further studies.

3.4. Optimization of analytical conditions

Fig. 4A showed the cyclic voltammetry (CV) of different deposition volumes of MWCNT on GCE. In the case of curve a, a well-defined oxidation peak (current of 56.53 μA and potential of 0.244 V) with peak-to-peak separation (ΔE_p 79 mV) was observed. The current response increased with the MWCNTs volume and reached a peak at 8 μL. Therefore, 8 μL was selected as the deposition volume of MWCNT.

In addition, the electrocatalytic activity of H_2O_2 on the modified electrode by linear sweep votlammograms (LSVs) was checked. The typical LSVs for 5 mmol L^{-1} H_2O_2 over the potential range of 0.0–1.0 V were showed in Fig. 4B. For MWCNT/GCE, no significant current was observed with potentials lower than 0.8 V. In the case of all Pt-Au/MWCNT/GC electrodes, increased catalytic current was observed after 0.3 V. The current enhanced with deposition time and maximum of catalytic current was obtained when the time of electrolytic deposition was 300 s

The concentration of ATCI was optimized in ECL detection solution (Fig. 5A). The ECL intensity was increased dramatically with ATCI concentrations from 1.5 to 2.0 mmol L^{-1} and then reached a plateau. Therefore, 2 mmol L^{-1} was selected as the optimal concentration of ATCI for the subsequent studies.

The concentration of luminol was one of the most influential parameters. With the concentration of luminol, the ECL peak intensity increased and reached the maximum at 0.4 mmol L^{-1} and then kept steady (Fig. 5B). Thus, 0.4 mmol L^{-1} was selected as the optimal concentration of luminol for further studies.

The ECL intensity of the proposed biosensor was also dependent on pH of the solution. With the pH, the ECL intensity increased, reaching the peak at pH 8.0 and then decreased (Fig. 5C). The optimum pH value for AChE was proved to be 8.0–9.0 and 7.0–8.0 for ChOx [22]. The enzyme lost activity irreversibly at higher

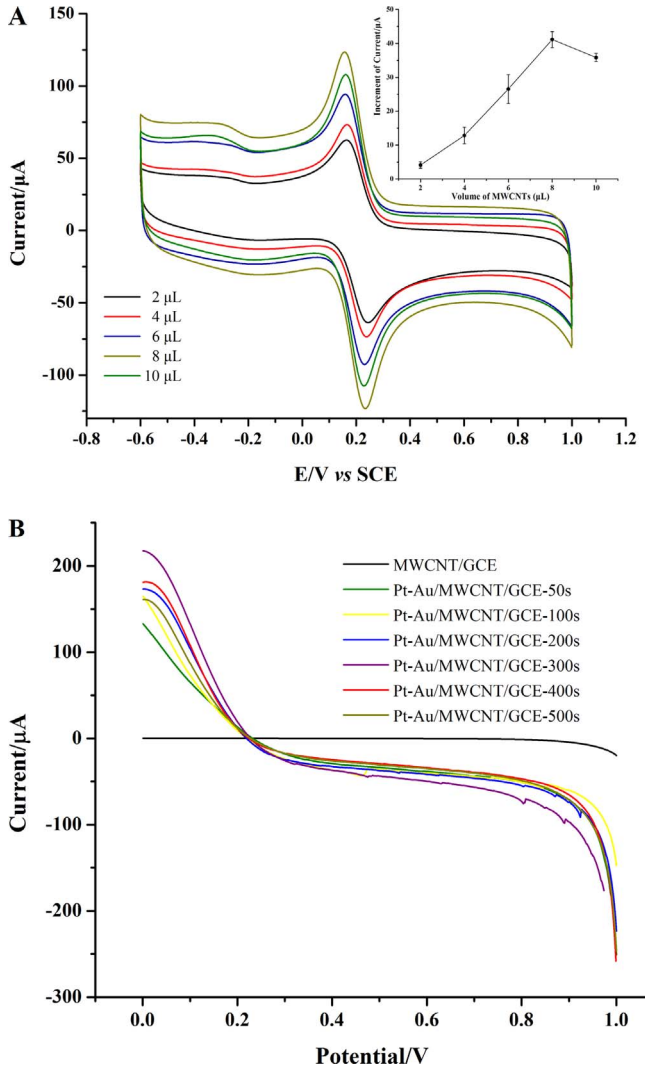

Fig. 4. Optimization of Pt-Au/MWCNT nanocomposites modified electrode. The CV responses of $Fe(CN)_6^{3-/4-}$ redox current through relevant MWCNTs volume deposited on the GCE (A) and the effect of the electrolytic deposition time toward the electrocatalytic reduction of H_2O_2 (B). Error bars are the standard error of the mean ($n=3$ electrodes).

pH because of the denaturation of the protein. Therefore, pH 8.0 was used as the supporting electrolyte for OPs detection.

3.5. Analytical performance of the proposed ECL biosensor for organophosphorous pesticides

The proposed biosensor was then used for determination of OPs under the optimized procedures. As expected, the ECL intensity decreased with the increasing concentration of inhibitor. The inhibition rate was calculated as follows:

$$\text{Inhibition}\quad (\%) = \left[\frac{I_0 - I_s}{I_0}\right] * 100 \tag{3}$$

Where I_0 was the ECL intensity without OPs inhibition, and I_s was the ECL intensity after the incubation of different inhibitor solutions for 10 min. When the inhibitor concentration was measured, the lower inhibition rate of enzyme activities should be avoided because some interferents could also inhibit the enzyme although the degree of the inhibition was very low. To avoid false positive occurrence, at least 10% inhibition rate of the enzyme activity is required [23]. Therefore, the limit of detection in this method was

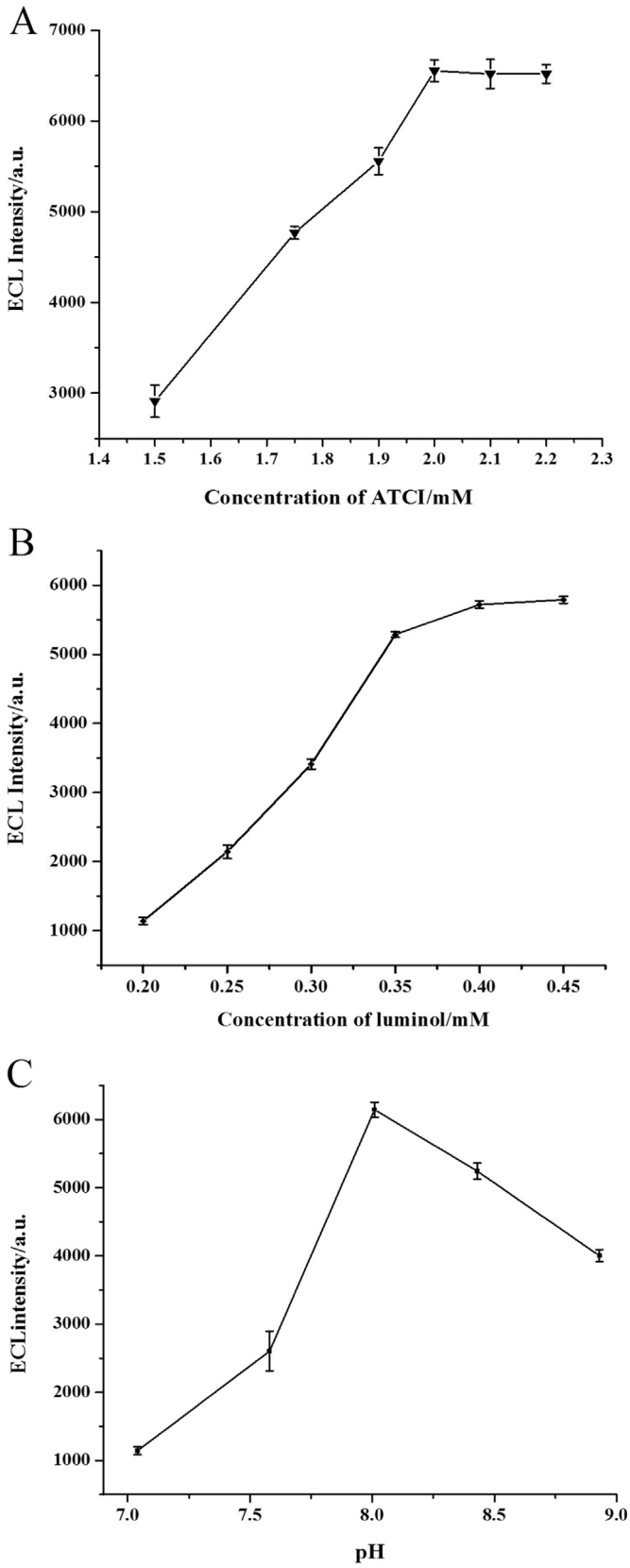

Fig. 5. (A) Effect of ATCI concentration on the ECL intensity with 0.4 mM luminol at AChE&ChOx/Pt-Au/MWCNT/GCE in 0.1 M PBS (pH 8.0). (B) Effect of luminol concentration on the ECL intensity with 2 mM ATCI at AChE&ChOx/Pt-Au/MWCNT/GCE in 0.1 M PBS (pH 8.0). (C) Effect of pH on the ECL intensity at AChE&ChOx/Pt-Au/MWCNT/GCE with 2 mM ATCI and 0.4 mM luminol.

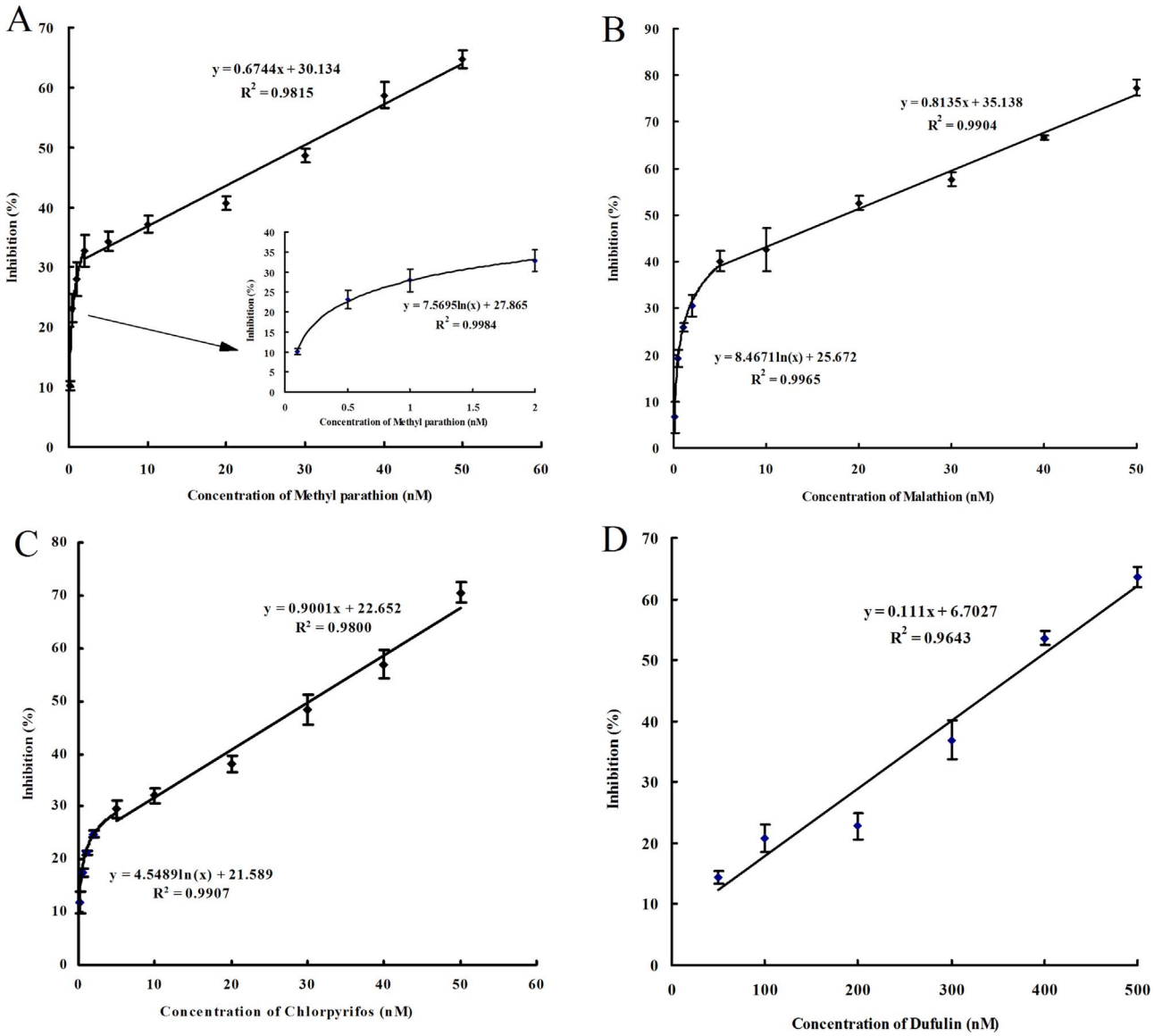

Fig. 6. Calibration curves for methyl parathion (A), malathion (B), chlorpyrifos (C), and dufulin (D) on the AChE&ChOx/Pt-Au/MWCNT/GCE. ECL conditions: scan rate: 100 mV/s; PMT voltage: 800 V.

defined as the concentration of the inhibitor needed to cause 10% inhibition of the enzyme activity. In a proposed method, four organophospohorous pesticides were individually determined. However, if four organophospohorous pesticides were detected simultaneously, they might interference each other as methyl parathion, malathion and chlopyrifos were the typical AChE inhibitors.

The calibration plot of inhibition for different pesticides was shown in Fig. 6. The calibration graph of the inhibition (%) versus the concentration of pesticide methyl parathion could be described by two sections, namely 0.1–2 nmol L^{-1} and 2–50 nmol L^{-1} (Fig. 6A). The obtained regression equations for the former and later were I (%)=7.5675ln$C$ (nmol L^{-1})+27.865 (R^2=0.9984) and I (%)=0.6744 C (nmol L^{-1})+30.134 (R^2=0.9815), respectively. Accordingly, the curves of I versus C toward pesticide malathion exhibited two ranges from 0.1 to 5 nmol L^{-1} and from 5 to 50 nmol L^{-1} with regression equations of I (%)=8.4671ln$C$ (nmol L^{-1})+25.672 (R^2=0.9965) and I (%)=0.8135C (nmol L^{-1})+35.138 (R^2=0.9904), respectively (Fig. 6B). For pesticide chlorpyrifos they were I (%)=4.5489ln$C$ (nmol L^{-1})+21.589 (R^2=0.9907) (0.1–5 nmol L^{-1}) and I (%)=0.9001C (nmol L^{-1})+22.652 (R^2=0.9800) (5–50 nmol L^{-1}), respectively (Fig. 6C). However, the linear working range of the biosensor for pesticide dufulin was found to be 50–500 nmol L^{-1}, with a regression equation of I (%)=0.111C (nmol L^{-1})+6.7027 (R^2=0.9643) (Fig. 6D). The inhibition (%) of AChE had a linear relationship with *ln* methyl parathion concentration from 0.1 to 2 nmol L^{-1} and a linear relationship with methyl parathion concentration from 2 to 50 nmol L^{-1}. However, the linear relationships were divided into two parts from 0.1 to 5 nmol L^{-1} and 5–50 nmol L^{-1} for chlorpyrifos and malathion. In addition, the IC_{50} (the concentration of the inhibitor needed to cause 50% inhibition of the enzyme activity) could be calculated from the regression equations. The IC_{50} was 30.38 nmol L^{-1} for chlorpyrifos, 29.46 nmol L^{-1} for methyl parathion and 18.27 nmol L^{-1} for malathion, respectively. The detection limit for methyl parathion, malathion, chlorpyrifos and dufulin was 0.09 nmol L^{-1}, 0.16 nmol L^{-1}, 0.08 nmol L^{-1}, and 29.7 nmol L^{-1}, respectively. Hence, the developed biosensor was highly sensitive and could be used to the individual detection of different OPs residues at the nmol L^{-1} level. The good analytical characteristics were attributed to the Pt-Au bimetallic nanoparticles on the surface of MWCNTs-

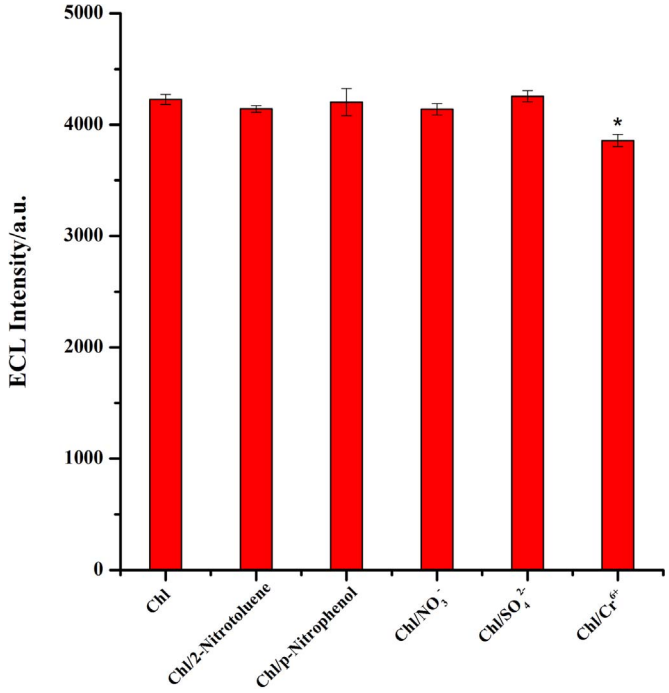

Fig. 7. Signals of 10 nmol L^{-1} chlorpyrifos in the absence and presence of 1 μmol L^{-1} 2-nitrotoluent, 1 μmol L^{-1} p-nitrophenol, 0.4 mM NO_3^-, 0.4 mM SO_4^{2-} and 0.4 mM Cr^{6+}, respectively. Vertical bars represent three replicate measurements ± standard deviations. *Asterisks* indicate the significant differences between in the absence and presence of Cr^{6+} ($p < 0.05$).

modified electrode, which provided high anchoring sites for the enzymes and good catalytic efficiency. Dufulin was selected as a reference in this study. However, its main functional mechanism was not towards AChE. The interaction between dufulin and AChE was weaker than that between the other three organophosphorous and AChE. Therefore, Dufulin shows a low sensitivity.

3.6. Selectivity of the biosensor

The selectivity and sensitivity of biosensor were investigated for the realistic application. A standard solution of pesticide chlorpyrifos in existing interfering species such as 2-nitrotoluene, p-nitrophenol, oxygen-containing inorganic ions (SO_4^{2-}, NO_3^-) and heavy metal ion Cr(VI) were analyzed (Fig. 7). Results showed that 100-fold concentrations of 2-nitrotoluene, p-nitrophenol, 40000-fold concentrations of SO_4^{2-}, and NO_3^- had negligible effects on chlorpyrifos detection by the present biosensor. In addition, Cr(VI) showed an 8.7% effect on inhibition, which was comparable to the earlier report [24]. These results clearly demonstrated that the proposed biosensor could selectively detect OPs and offer a credible signal when the interfering species reached a relatively high concentration.

3.7. Regeneration of acetylcholinesterase

It has been proved that the inhibition of AChE by OPs was irreversible because of the covalent link of organophosphorus-based pesticides to AChE [38]. However, AChE was reactivated by the usage of nucleophilic compound 2-pyridine aldoxime methiodide (2-PAM). The regeneration of AChE activity could reach to 90% of the original activity after a 15 min incubation in the PBS of 2-PAM. This reactivation further confirmed that the inhibition was due to the pesticides and the biosensor was renewed.

Table 1.
Recoveries of cabbage spiked with organophosphorous pesticides.

Compound	Cabbage		Recovery (%)	RSD[a] (%)
	Spiked (nmol kg^{-1})	Found (nmol kg^{-1})		
Chlorpyrifos	0	nd[b]		
	10	9.92	99.19	8.43
	40	35.95	89.88	3.71
	100	95.15	95.15	5.41
Malathion	0	nd[b]		
	10	9.94	99.36	5.42
	40	43.37	108.43	7.18
	100	95.95	95.95	9.92
Methyl parathion	0	nd[b]		
	10	9.61	96.04	1.78
	40	36.69	91.73	7.86
	100	97.19	97.19	9.54
Dufulin	0	nd[b]		
	100	77.69	77.69	11.14
	250	221.63	88.65	7.38
	500	402.55	80.51	8.59

[a] RSD relative standard deviatio.
[b] nd: not detected.

3.8. Analysis of pesticides in cabbage sample

To evaluate the precision and application of the proposed method in matrix or additive interferences, cabbages were collected and analyzed by the ECL biosensor using a standard addition method. The cabbage samples without addition of OPs were also evaluated. As summarized in Table 1, the concentration of original samples was not detected. The recoveries for the cabbage samples were found to be 77.69–108.43%, with RSD values ranging from 1.78–11.14%, respectively. Therefore, the preliminary results indicated that the proposed method can be used for individual determination of different OPs residues in real samples with high accuracy and reproducibility.

The method was further compared to other literatures with regard to the detection of OPs in complex matrices [24,39–41]. The recoveries of OPs in the proposed method were comparable to the previous reports (Table 2). The limit detection for the representative OPs (methyl parathion, malathion and chlorpyrifos) was 24–52 ng kg^{-1}. Obviously, the limitation was significantly lower or comparable with the previous reports.

4. Conclusions

A novel ECL biosensor for determination of organophosphorous pesticides has been developed. The proposed biosensor consisted of AChE&ChOx enzyme composites which were immobilized on the surface of Pt-Au/MWCNT modified glass carbon electrode through the cross-linking by cysteine. Based on the integration of these electrochemically nanometer materials and the generation of coreactant H_2O_2 in enzymatic reaction, the ECL signal of luminol was significantly amplified. The resulting biosensor showed good sensitivity and long-term stability when used for realistic samples. Significant advantages of the proposed biosensor include simplicity of construction, the benefit of the enhancement effects of the nanoparticles (MWCNTs, Pt, and Au) and enzyme composites on the ECL intensity of luminol in the luminol-ECL system. More importantly, the biosensor also showed fine applicability for the

Table 2.
Comparison of analytical performances of different organophosphorous pesticides biosensors.

Matrices	Detection method	Working electrode	Analytes	Recovery (%)	Detection limit	Reference
Cabbage	ECL	AChE&ChOx/Pt-Au/MWCNT/GCE	OP pesticides	78–108	0.08–29.7 nmol L^{-1}	Our work
Water	Amperometric	AChE/Fe_3O_4/c-MWCNT/Au electrode	OP insecticides	95–109	0.1–10 nmol L^{-1}	24
Cabbage	ECL	AChE–QDs–GNs–GCE	Methyl parathion	94–103	60 ng L^{-1} (0.23 nmol L^{-1})	41
Milk	Amperometric	screen-printed thick-film electrodes	Paraoxon, Carbaryl	89–107	1, 20 μg L^{-1} (3.63, 99.39 nmol L^{-1})	39
–	Amperometric	MPDE-CdTe/Cys/Au/MWCNT/GCE	Methyl parathion	–	1 ng mL^{-1} (3.80 nmol L^{-1})	40

QDs, quantum dots.
MPDE, methyl parathion degrading enzyme.

individual detection of different OPs in realistic samples. Thus, our study represents a novel, simple and sensitive method for monitoring the trace OPs in environmental media.

Acknowledgements

The authors acknowledge the financial support of the National Natural Science Foundation of China (Nos. 21377058, 21577064) and the financial support of the Special Fund for Agro-scientific Research in the Public Interest (No. 201203022) from the Ministry of Agriculture of China.

References

[1] B.K. Singh, A. Walker, Microbial degradation of organophosphorus compounds, FEMS Microbiol. Rev. 30 (3) (2006) 428–471.
[2] L.M. Wang, D.L. Lu, J. Wang, D. Du, Z.X. Zou, H. Wang, J.N. Smith, C. Timchalk, F. Q. Liu, Y.H. Lin, A novel immunochromatographic electrochemical biosensor for highly sensitive and selective detection of trichloropyridinol, a biomarker of exposure to chlorpyrifos, Biosens. Bioelectron. 26 (6) (2011) 2835–2840.
[3] Y.H. Qu, H. Min, Y.Y. Wei, F. Xiao, G.Y. Shi, X.H. Li, L.T. Jin, Au-TiO_2/Chit modified sensor for electrochemical detection of trace organophosphates insecticides, Talanta 76 (2008) 758–762.
[4] W.J. Hayes, E.R. Laws, Handbook of Pesticide Toxicology: Classes of Pesticides (EDs), Academic Press, San Diego, 1991.
[5] X.D. Hua, G.L. Qian, J.F. Yang, B.S. Hu, J.Q. Fan, N. Qin, G. Li, Y.Y. Wang, F.Q. Liu, Development of an immunochromatographic assay for the rapid detection of chlorpyrifos-methyl in water samples, Biosens. Bioelectron. 26 (1) (2010) 189–194.
[6] K. Seebunrueng, Y. Santaladchaiyakit, P. Soisungnoen, S. Srijaranai, Catanionic surfactant ambient cloud point extraction and high-performance liquid chromatography for simultaneous analysis of organophosphorus pesticide residues in water and fruit juice samples, Anal. Bioanal. Chem. 401 (5) (2011) 1703–11712.
[7] S.N. Sinha, R. Pal, A. Dewan, M.M. Mansuri, H.N. Saiyed, Effect of dissociation energy on ion formation and sensitivity of an analytical method for determination of chlorpyrifos in human blood, using gas chromatography–mass spectrometer (GC–MS in MS/MS), Int. J. Mass Spectrom. 25 (2006) 348–357.
[8] L. Gámiz-Gracia, A.M. García-Campaña, J.J. Soto-Chinchilla, J.F. Huertas-Pérez, A. González-Casado, Analysis of pesticides by chemiluminescence detection in the liquid phase, Trends Anal. Chem. 24 (11) (2005) 927–942.
[9] K. Futagami, C. Narazaki, Y. Kataoka, H. Shuto, R. Oishi, Application of high-performance thin-layer chromatography for the detection of organophosphorus insecticides in human serum after acute poisoning, J. Chromatogr. B 704 (1997) 369–373.
[10] J.J. Zhang, T.F. Kang, Y.C. Hao, L.P. Lu, S.Y. Cheng, Electrochemiluminescent immunosensor based on CdS quantum dots for ultrasensitive detection of microcystin-LR, Sens. Actuators B 214 (2015) 117–123.
[11] P.P. Joshi, S.A. Merchant, Y.D. Wang, D.W. Schmidtke, Amperometric biosensors based on redox polymer-carbon nanotube-enzyme composites, Anal. Chem. 77 (2005) 3183–3188.
[12] S.M. Wang, L. Ge, X.R. Song, J.H. Yu, S.G. Ge, J.D. Huang, F. Zeng, Paper-based chemiluminescence ELISA: Lab-on-paper based on chitosan modified paper device and wax-screen-printing, Biosens. Bioelectron. 31 (1) (2012) 212–218.
[13] M.M. Richter, Electrochemiluminescence, Chem. Rev. 104 (6) (2004) 3003–3036.
[14] H.F. Li, C.G. Xie, X.C. Fu, Electrochemiluminescence sensor for sulfonylurea herbicide with molecular imprinting core-shell nanoparticles/chitosan composite film modified glassy carbon electrode, Sens. Actuators B 181 (2013) 858–866.
[15] A. Sassolas, L.J. Blum, B.D. Leca-Bouvier, Electrogeneration of polyluminol and chemiluminescence for new disposable reagentless optical sensors, Anal. Bioanal. Chem. 390 (2008) 865–871.
[16] J.P. Li, S.H. Li, X.P. Wei, H.L. Tao, H.C. Pan, Molecularly imprinted electrochemical luminescence sensor based on signal amplification for selective determination of trace gibberellin A3, Anal. Chem. 84 (2012) 9951–9955.
[17] G.F. Jie, B. Liu, H.C. Pan, J.J. Zhu, H.Y. Chen, CdS nanocrystal-based electrochemiluminescence biosensor for the detection of low-density lipoprotein by increasing sensitivity with gold nanoparticle amplification, Anal. Chem. 79 (2007) 5574–5581.
[18] M.S. Wu, H.W. Shi, L.J. He, J.J. Xu, H.Y. Chen, Microchip device with 64-site electrode array for multiplexed immunoassay of cell surface antigens based on electrochemiluminescence resonance energy transfer, Anal. Chem. 84 (9) (2012) 4207–4213.
[19] G.M. Nie, Z.M. Bai, W.Y. Yu, J. Chen, Electrochemiluminescence biosensor based on conducting poly(5-formylindole) for sensitive detection of ramos cells, Biomacromolecules 14 (2013) 834–840.
[20] H.H. Chu, W.Y. Guo, J.W. Di, Y. Wu, Y.F. Tu, Study on sensitization from reactive oxygen species for electrochemiluminescence of luminol in neutral medium, Electroanalysis 21 (14) (2009) 1630–1635.
[21] H. Cui, W. Wang, C.F. Duan, Y.P. Dong, J.Z. Guo, Synthesis, characterization, and electrochemiluminescence of luminol-reduced gold nanoparticles and their application in a hydrogen peroxide sensor, Chem. Eur. J. 13 (24) (2007) 6975–6984.
[22] X.P. Wu, X. Zhong, Y.Q. Chai, R. Yuan, Electrochemiluminescence acetylcholine biosensor based on biofunctional AMs-AChE-ChO biocomposite and electrodeposited graphene-Au-chitosan nanocomposite, Eletrochim. Acta 147 (2014) 735–742.
[23] N. Jha, S. Ramaprabhu, Development of Au nanoparticles dispersed carbon nanotube-based biosensor for the detection of paraoxon, Nanoscale 2 (5) (2010) 806–810.
[24] N. Chauhan, C.S. Pundir, An amperometric biosensor based on acetylcholinesterase immobilized onto iron oxide nanoparticles/multi-walled carbon nanotubes modified gold electrode for measurement of organophosphorus insecticides, Anal. Chim. Acta 701 (2011) 66–74.
[25] A.A. Ciucu, C. Negulescu, R.P. Baldwin, Detection of pesticides using an amperometric biosensor based on ferophthalocyanine chemically modified carbon paste electrode and immobilized bienzymatic system, Biosens. Bioelectron. 18 (2003) 303–310.
[26] S. Upadhyay, G.R. Rao, M.K. Sharma, B.K. Bhattacharya, V.K. Rao, R. Vijayaraghavan, Immobilization of acetylcholineesterase-choline oxidase on a gold-platinum bimetallic nanoparticles modified glassy carbon electrode for the sensitive detection of organophosphate pesticides, carbamates and nerve agents, Biosens. Bioelectron. 25 (2009) 832–838.
[27] C.E. Banks, R.G. Compton, Edge plane pyrolytic graphite electrodes in electroanalysis: an overiew, Anal. Sci. 21 (2005) 1263–1268.
[28] Z.Y. Lin, L.Z. Huang, Y. Lin, J.M. Lin, Y.W. Chi, G.N. Chen, Electrochemiluminescent biosensor based on multi-wall carbon nanotube/nano-Au modified electrode, Electrochem. Commun. 10 (2008) 1708–1711.
[29] H.F. Cui, J.S. Ye, X. Liu, W.D. Zhang, F.S. Sheu, Pt–Pb alloy nanoparticle/carbon nanotube nanocomposite: a strong electrocatalyst for glucose oxidation, Nanotechnology 17 (2006) 2334–2339.
[30] Y.J. Yang, S.S. Hu, Electrodeposited MnO_2/Au composite film with improved electrocatalytic activity for oxidation of glucose and hydrogen peroxide, Eletrochim, Acta 55 (2010) 3471–3476.
[31] H. Cui, Y. Xu, Z.F. Zhang, Multichannel electrochemiluminescence of luminol in neutral and alkaline aqueous solutions on a gold nanoparticle self-assembled electrode, Anal. Chem. 76 (14) (2004) 4002–4010.
[32] H.H. Chu, Y. Wu, Y.F. Tu, Sensitization of the electrochemiluminescence of luminol from platinum sol modified electrode, Chin. J. Anal. Chem. 34 (9) (2006) 1303–1306.
[33] Y.K. Yang, G.Z. Fang, G.Y. Liu, M.F. Pan, X.M. Wang, L.J. Kong, X.L. He, S. Wang, Electrochemical sensor based on molecularly imprinted polymer film via sol–gel technology and multi-walled carbon nanotubes-chitosan functional layer for sensitive determination of quinoxaline-2-carboxylicacid, Biosens. Bioelectron. 47 (2013) 475–481.
[34] J.H. Chen, Z.H. Zhang, L.J. Luo, S.Z. Yao, Surface-imprinted chitosan-coated magnetic nanoparticles modified multi-walled carbon nanotubes biosensor for detection of bovine serum albumin, Sens. Actuators B 163 (2012) 76–83.
[35] Y.J. Zou, C.L. Xiang, L.X. Sun, F. Xu, Glucose biosensor based on electrodeposition of platinum nanoparticles onto carbon nanotubes and immobilizing enzyme with chitosan-SiO_2 sol–gel, Biosens. Bioelectron. 23 (2008) 1010–1016.

[36] C.B. Liu, K. Wang, S.L. Luo, Y.H. Tang, L.Y. Chen, Direct electrodeposition of graphene enabling the one-step synthesis of graphene-metal nanocomposite films, Small 7 (9) (2011) 1203–1206.
[37] N. Zhu, H. Gao, Q. Xu, Y. Lin, L. Su, L. Mao, Sensitive impedimetric DNA biosensor with poly(amidoamine) dendrimer covalently attached onto carbon nanotube electronic transducers as the tether for surface confinement of probe DNA, Biosens. Bioelectron. 25 (6) (2010) 1498–1503.
[38] L.G. Sultatos, Mammalian toxicology of organophosphorus pesticides, J. Toxicol. Environ. Health 43 (1994) 271–289.
[39] Y. Zhang, S.B. Muench, H. Schulze, R. Perz, B. Yang, R.D. Schmid, T.T. Bachmann, Disposable biosensor test for organophosphate and carbamate insecticides in milk, J. Agric. Food Chem. 53 (13) (2005) 5110–5115.
[40] D. Du, W.J. Chen, W.Y. Zhang, D.L. Liu, H.B. Li, Y.H. Lin, Covalent coupling of organophosphorus hydrolase loaded quantum dots to carbon nanotube/Au nanocomposite for enhanced detection of methyl parathion, Biosens. Bioelectron. 25 (2010) 1370–1375.
[41] H. Liang, D.D. Song, L.M. Gong, Signal-on electrochemiluminescence of biofunctional CdTe quantum dots for biosensing of organophosphate pesticides, Biosens. Bioelectron. 53 (2014) 363–369.